Available online at www.derpharmachemica.com

Scholars Research Library

Der Pharma Chemica, 2015, 7(10):128-138
(http://derpharmachemica.com/archive.html)

ISSN 0975-413X
CODEN (USA): PCHHAX

DFT investigations on optoelectronic properties of new low gap compounds based on pyran as solar cells materials

A. El Assyry[1], A. Hallaoui[2], A. Zarrouk[3], M. El Hezzat[4], M. Assouag[5], S. Boukhris[6] and M. M. Ebn Touhami[7]

[1]*Laboratoire d'Optoélectronique et de Physico-chimie des Matériaux, (Unité associée au CNRST), Université Ibn Tofail, Faculté des Sciences, Kenitra, Morocco*
[2]*Poly-disciplinary Faculty of Taza, Taza Gare, Morocco*
[3]*LCAE-URAC18, Faculty of Science, Mohammed first University, Oujda, Morocco*
[4]*Laboratoire de Physico-Chimie des Matériaux Vitreux et Cristallisés, Faculté des Sciences, Université Ibn Tofail, kenitra, Morocco*
[5]*Equipe Matériaux Avancés et Applications ENSAM, Université Moulay Ismail, Al Mansour, Meknès, Morocco*
[6]*Laboratoire de Chimie Organique, Organométallique et Théorique, Faculté des Sciences, Université Ibn Tofail, kenitra, Morocco*
[7]*Ingénierie des Matériaux et d'Environnement: Modélisation et application, Faculté des Sciences, Université Ibn Tofail, Kenitra, Morocco*

ABSTRACT

Theoretical study by using DFT method on four compounds based on Ethyl 2-methyl-3-carboxylate-4-phenyl-4H-5-cyano-6-amino-pyran is reported in this paper; one adding the Cl, CH_3 and NO_2 substituent for one of the most electronegative positions of the phenyl ring. The aim is to investigate their effects on the electronic structure and the optoelectronics properties. The time-dependent DFT (TD-DFT/CAM-B3LYP /6-31G(d,p)) level has been used for predict the excitations properties. The theoretical knowledge of the HOMO and LUMO energy levels of the components is cannot be ignored in investigating suitable materials for organic solar cells; so the HOMO, LUMO, the gap energy, the V_{oc} (open circuit voltage) and λ_{max} of absorption and other quantum parameters of the studied compound have been calculated and reported. These properties suggest these materials as good candidates for organic solar cells.

Keywords: Pyrane, Solar cells, DFT, Electronic properties, HOMO, LUMO, Gap energy.

INTRODUCTION

The development of the using of the energy over last decade brought the scientists to research other sources of the energy such as the conversion of solar energy to electric energy via solar cells, among this solar cells we can find bulk heterojunction (BHJ) which is based on the conjugated molecules able to absorb two or more photons and going easily to their excited states. Recently the conjugated molecules have been the subject of much research due to the growing interest in advanced photonic applications, low-cost, flexible and lightweight materials such as batteries [1], electroluminescent devices [2], field-effect transistors [3] and photovoltaics [4]. Power conversion efficiency (PCE) of organic solar cells, which had been too low for applications (0.001 to 0.01%) when made with a pure conjugated polymer, poly(3-hexylthiophene), increased up to ~5% with the introduction of fullerene-derivative photoelectron acceptors (phenyl C61 or C71 butyric acid methyl ester; PCBM) in the photoelectron-donating matrix of the conjugated polymer for interpenetrating donor acceptor network in a bulk phase, a so-called bulk heterojunction (BHJ) network [5-11]. Conjugated molecules or polymers containing thiophene moieties either in the

main or side chains have attracted much attention because of their unique electronic properties, their high photoluminescence quantum efficiency, thermal stability and also their facile color tenability [12]. These properties depend on the degree of electronic delocalization in these materials and on the modification of chemical structure through the incorporation of charge carriers. In order to obtain materials with more predominant capability, the development of novel structures is now being undertaken following the molecular engineering guidelines. This strategy has given rise to a wide range of applications such as transparent conductors, light-emitting materials [13-15].

In the past few years, several groups of chemists proposed new polymer structures as alternatives of P3HT and MDMOPPV; the performances of these two polymers are characterized by their relatively large band gap [13]. For many years, Internal Charge Transfer (ICT) from an electron-rich unit to an electron deficient unit has been extensively used to obtain the low band gap of the conjugated molecules [16-22]. By using the ICT strategy, new polymers have been developed to better harvest the solar spectrum, especially in the 1.4-1.9 eV region. Several low band gap polythiophene derivatives have been reported by Reynolds [23, 24], and Krebs [25], but until now, relatively low performances in solar cells have been obtained.

The HOMO and LUMO energy levels of the donor and acceptor compounds in photovoltaic devices are very important factors to determine the effective charge transfer will happen between donor and acceptor. The offset of band edges of the HOMO and LUMO levels will prove responsible for the improvement of all photovoltaic properties of the organic solar cells.

This work, include the theoretical analysis of the geometries and electronic properties of new conjugated compounds based on pyran (P1, P2, P3 and P4) (see Fig. 1). The theoretical ground-state geometry and electronic structure of the studied molecules were investigated by the DFT method at B3LYP level with 6-31 G (d, p) basis set. The effects of the ring structure and the substituent on the geometries and electronic properties of these materials were discussed in the aim to elucidate the relationship between molecular structure and optoelectronic properties. This investigation was used to drive next synthesis towards compounds more useful as active materials in optoelectronic. The theoretical knowledge of the HOMO and LUMO energy levels of the components is basic in studying organic solar cells so the HOMO, LUMO, gap energy and V_{oc} (open circuit voltage) of the studied compounds have been calculated and reported.

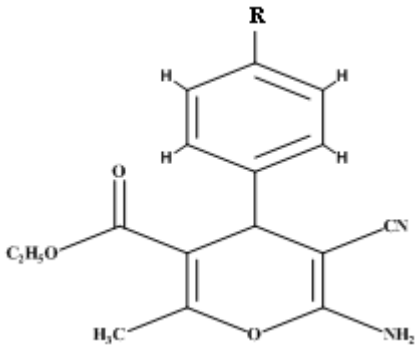

Composed	R
P1	H
P2	Cl
P3	CH_3
P4	NO_2

Figure 1: The sketch map of studied structures

MATERIALS AND METHODS

Theoretical background

For the short-circuit current density J_{sc} in dye-sensitized solar cells DSSC, it is determined as:

$$J_{sc} = \int_{\lambda} LHE(\lambda)\Phi_{inject}\eta_{collect}d\lambda$$

where $LHE(\lambda)$ is the light harvesting efficiency, Φ_{inject} is the electron injection efficiency, and $\eta_{collect}$ is the charge collection efficiency. For the same DSSC with only different dyes, it is reasonable to assume that the $\eta_{collect}$ is a constant. As a result, to shed light onto the relationship between the J_{sc} and η theoretically, we investigated the *LHE*, Φ_{inject} and total reorganization energy (λ_{total}). From Eq. (2), to obtain a high J_{sc}, the efficient sensitizers applied in DSSC should have a large *LHE*, which can be expressed as [26]:

$$LHE = 1 - 10^{-f}$$

where f is the oscillator strength of the dye associate to the wavelength λ_{max} in the equation. We noticed that the larger oscillating strength obtained, the higher light-harvesting efficiency will have. At the same time, a large Φ_{inject} could also guarantee a high J_{sc}, which is related to the injection driving force ΔG^{inject} and evaluated by [26]:

$$\Delta G^{inject} = E^{dye*} + E_{CB}$$

where E^{dye*} is the oxidation potential energy of the dye in the excited state and E_{CB} is the reduction potential of the conduction band of TiO_2, respectively. There, we use in this work $E_{CB} = -4.0$ eV for TiO_2 [27], which is widely used in some papers [28-30], and the E^{dye*} can be estimated [29-31] by:

$$E^{dye*} = E^{dye} - E_{00}$$

where E^{dye} is the oxidation potential energy of the dye in the ground state, while E_{00} is an electronic vertical transition energy corresponding to the λ_{max}. It is generally accepted that there are two schemes to evaluate the ΔG^{inject}, which is relaxed and unrelaxed paths. The previous works concluded that the calculation with the unrelax path is reliable [29, 30]. Thus, the electron injection from excited state of dye to the TiO_2 (CB) is determined by the unrelax path in our investigation.

Additionally, the small total reorganization energy (λ_{total}) which contains the hole and electron reorganization energy could enhance the J_{sc}. Namely, the smaller λ_{total} value obtained, the faster charge-carrier transport rates will be [26]. So we computed the hole and the electron reorganization energy (λ_h and λ_e) according to the following formula [32]:

$$\lambda_i = \left(E_0^{\pm} - E_{\pm}^{\pm}\right) + \left(E_{\pm}^{0} - E_0\right)$$

where $E_0^{\pm}$ is the energy of the cation or anion calculated with the optimized structure of the neutral molecule, $E_{\pm}^{\pm}$ is the energy of the cation or anion calculated with the optimized cation or anion structure, $E_{\pm}^{0}$ is the energy of the neutral molecule calculated at the cationic or anionic state, and the E_0 is the energy of the neutral molecule at ground state.

In real devices, the circuit must be modified to account for serial R_s and shunt R_{sh} resistance losses. An 'ideality factor' n is also introduced (it is 1 for an ideal diode). I_s is the saturation current under reverse bias, I_L is a current source whose intensity depends on G. R_L is the charge resistance. Currents become determined by the Equation [33]:

$$I\left(1 + \frac{R_s}{R_{sh}}\right) - \frac{V}{R_{sh}} + I_L = I_s\left(\exp\left(\frac{e}{nkT}(V - IR_s)\right) - 1\right)$$

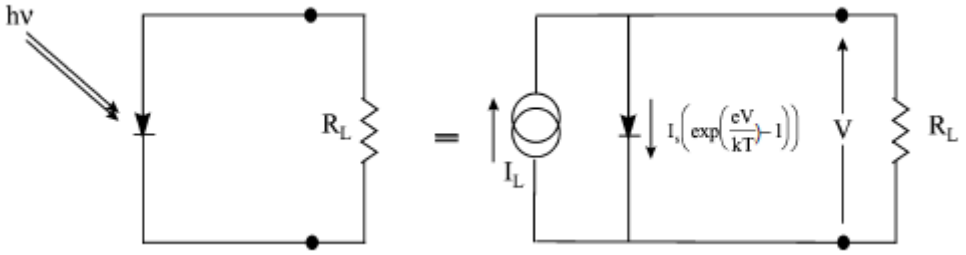

Figure 2: Equivalent circuit of an ideal cell under light

The short circuit current I_{sc} is the one which crosses the cell at zero applied voltage; it is a function of illumination G. Series resistance depends on the material's resistivity, the electrodes resistivity, and the metal-organic interfaces at the electrodes. The shunt resistance (several kΩ) corresponds to leaks and shorts in the diode. The slope around zero bias is a measure of the shunt resistance [34]. The relation between V_{oc} and I_{sc} can be determined when it is assumed that: $R_s = 0$ and $R_{sh} = \infty$, with $I = 0$ and $I_L = I_{sc}$:

$$V_{oc} = \frac{nkT}{e} \ln\left(\frac{I_{sc}}{I_{so}} + 1\right)$$

A small shunt resistance R_{sh} will reduce V_{oc}. Additionally; the cell will not deliver any voltage under low illumination G. I_{sc} is essentially reduced by the series resistance R_s.

Methodology

All our calculations were performed in the gas phase by using the quantum method DFT (Density Functional Theory) with the hybrid functional of exchange correlation B3LYP [35, 37] (Becke three-parameter Lee–Yang–Parr) and the basis sit used for all atoms over all calculations is always the basis set of people with dual-polarized (6-31G (d, p)) [38]. All the optimizations were done without constraint on dihedral angles. The predict energy of excited state and oscillator strengths (f) were investigated by using TD-DFT/CAM-B3LYP calculations in chloroform solvent on the fully DFT optimized geometries. We have also examined HOMO, LUMO levels and the energy; the used software of all calculations is Gaussian 09 program [39].

RESULTS AND DISCUSSION

Geometry Structures

The chemical structures of the pyrane derivatives compounds used in this work are depicted in Table 1. All the molecular geometries have been calculated with the B3LYP/6-311G(d,p) level. It was found in other works that the DFT-optimized geometries were in excellent agreement with the data obtained from X-ray analysis [40-42]. The optimized geometries of all studied molecules (P1, P2, P3 and P4) are shown in Fig. 3, and the selected bond lengths, bond angles and dihedral angles of compounds in the ground state are listed in Table 1. We believe that this coplanar molecular-structure should improve the electron transfer from the electron-donor to the electron acceptor through the π-spacer unit for these dyes. For each model, the calculated critical bond lengths of Pi (i = 1–4) in all the ground state (S_0) are compared in Table 1. These results indicate that the connection of acceptor group and the π-bridge is crucial for highly enhanced intramolecular charge transfer (ICT) character, which is important for the absorption spectra red-shift.

Table 1: Geometrical parameters for compounds in Fig. 1 optimized at the B3LYP/6-31G (d,p) level of theory.

Bond length r(Å)				Bond angle θ(°), dihedral τ(°)			
P1		**P2**		**P1**		**P2**	
r(CC) phenyl ring	1.3933	$r(C_{20}Cl_{21})$	1.76	θ(CCC) phenyl ring	120.20	$\theta(C_{18}C_{20}Cl_{21})$	116.73
r(CH) phenyl ring	1.07			θ(CCH) phenyl ring	116.48		
$r(O_1C_2)$	1.3946	**P3**		$\theta(O_1C_2C_3)$	120.20	**P3**	
$r(C_2C_3)$	1.3933	$r(C_{20}C_{21})$	1.54	$\theta(C_2C_3C_{11})$	116.14	$\theta(C_{18}C_{20}C_{21})$	116.73
$r(C_3C_4)$	1.4023	$r(C_{21}H_{38})$	1.07	$\theta(C_3C_{11}O_{12})$	130.07	$\theta(C_{20}C_{21}H_{38})$	109.47
$r(C_4C_{15})$	1.4618			$\theta(C_3C_{11}O_{13})$	112.29	$\tau(C_{18}C_{20}C_{21}H_{39})$	-170.65
$r(C_3C_{11})$	1.54			$\theta(C_{11}O_{13}C_{31})$	110.60	$\tau(C_{18}C_{20}C_{21}H_{40})$	-50.65
$r(C_{11}O_{12})$	1.2302			$\theta(C_5C_6N_{28})$	118.96		
$r(C_{11}O_{13})$	1.3569	**P4**		$\theta(C_6N_{28}H_{29})$	109.47	**P4**	
$r(O_{13}C_{31})$	1.43	$r(C_{20}N_{21})$	1.47	$\theta(C_4C_5C_{26})$	123.50	$\theta(C_{20}N_{21}O_{38})$	118.39
$r(C_5C_{26})$	1.54	$r(N_{21}O_{38})$	1.2376	$\tau(C_6C_5C_4C_3)$	0.06	$\theta(C_{20}N_{21}O_{39})$	118.39
$r(C_{26}N_{27})$	1.16			$\tau(C_7C_2O_1C_6)$	-178.64	$\tau(C_{18}C_{20}N_{21}H_{38})$	95.50
$r(C_6N_{28})$	1.47			$\tau(H_8C_7C_2O_1)$	125.11	$\tau(C_{18}C_{20}N_{21}H_{39})$	-84.49

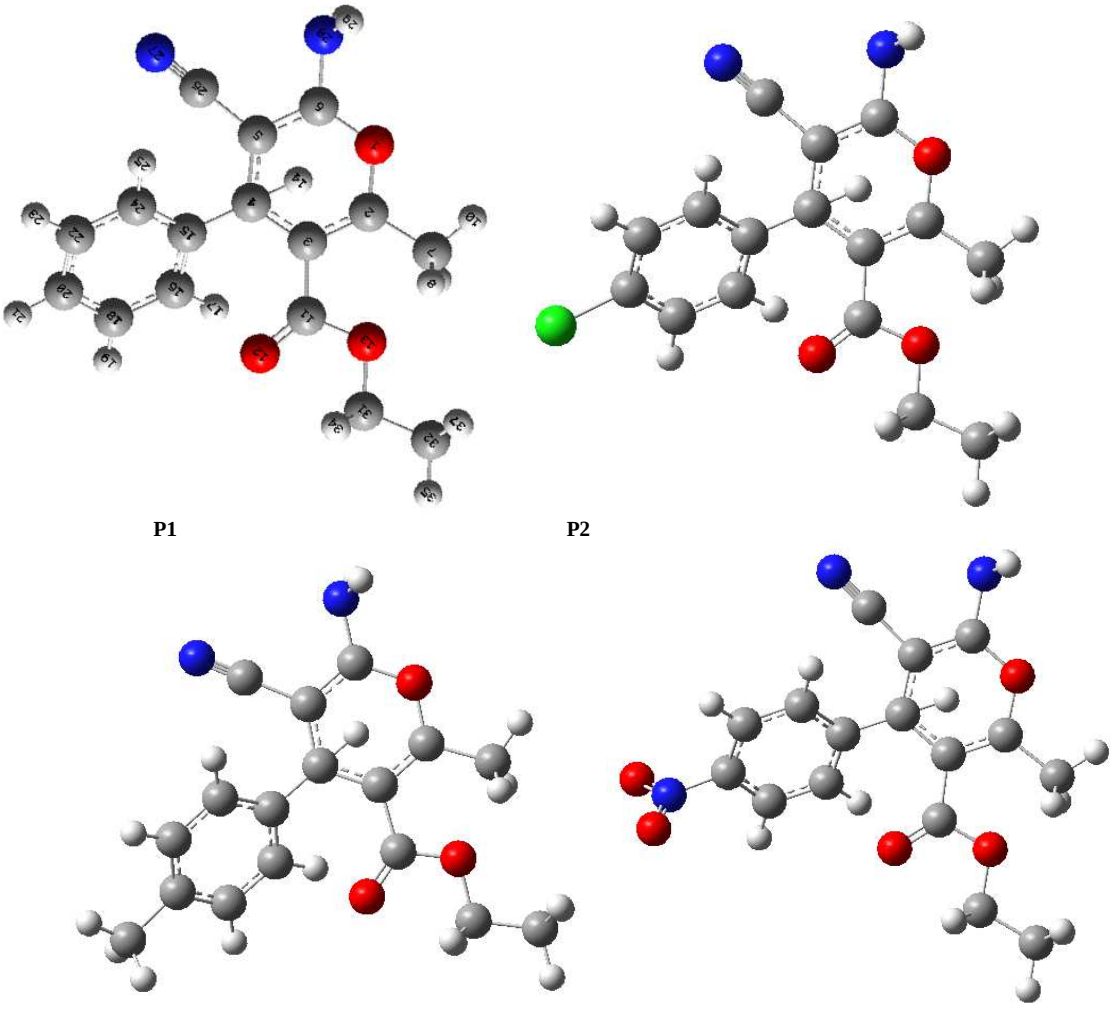

P1 **P2**

P3 **P4**

Figure 3: Optimized structure at B3LYP/6-31G (d,p) level for Pi (i=1-4) compounds

Quantum chemical parameters

One of the most important features of metal-free organic sensitizers in DSSC is the ICT from donor to acceptor/anchoring group. The ICT behavior was obtained from the frontier molecular orbital (FMO) contribution [43, 44]. The one most important property in the materials organic is the energy gap in which it can affect the photocurrent of the compound. Mostly smaller band gap of this compound lead to the ease of transporting electrons from HOMO level to LUMO level over the absorbing of the wavelength light. Moreover, the HOMO displays an anti-bonding character between two adjacent fragments and bonding character within each unit. The LUMOs exhibit the bonding character between the two adjacent fragments, so the lowest lying singlet states are corresponding to electronic transition of π–π* type [45, 46]. Table 2 illustrate the values of HOMO, LUMO orbital's and gap energies of all compounds (P1, P2, P3 and P4) which are (-5.340, -5.231, -5.313, -5.285 eV); (-3.978, -3.981, -3.979, -3.980 eV); (1.362, 1.250, 1.334, 1.305 eV) respectively. The increasing of the intra-molecular charge transfer (ICT) characters of all molecules (P1, P2, P3 and P4) lead to stabilize of the energy of HOMO and LUMO and also lead to a decrease the gap between HOMO and LUMO, which would make the organic photovoltaic (OPV) spectra red shifted. We can also remark that the order of energy gap between HOMO and LUMO is: P2<P4<P3<P1. By comparing the values of gap energies of these compounds between them, we remark that when going from P2-P4 to P3-P1, the energy gap increases. This is often attributed to the effect of the conjugated system and aromaticity of the studied compounds. Finally, the values of energy gap for four compounds (P1, P2, P3 and P4) are much smaller without exception. These four compounds with this lowest energy gap are expected to have most outstanding photophysical properties. The Frontier molecular orbital FMO of all compounds have analogous distribution characteristics. All HOMOs show the typical aromatic features with electron delocalization for the whole conjugated molecule. The LUMOs are mainly concentrated on electron-deficient unit and the right of molecular chain. In other hand we remark that the HOMO orbital of all compounds presents a bonding character, whereas the LUMO orbital of all compounds presents an anti-bonding character (Fig.4). Table 2 also present the total energy (E_T), dipole moment (μ), nuclear repulsion energy (E_{NN}) and Electronic spatial extent (ESE).

Table 2: Electrical and optical parameters for all compounds obtained by B3LYP/6-31G (d, p) level

compound	E_{LUMO} (eV)	E_{HOMO} (eV)	E_g (eV)	E_T (eV)	μ (Debye)	E_{NN} (Hartree)	ESE (au)
P1	-3.978	-5.340	1.362	-25818	7.637	1657	6355
P2	-3.981	-5.231	1.250	-38264	9.642	1888	8309
P3	-3.979	-5.313	1.334	-26882	7.403	1783	7363
P4	-3.980	-5.285	1.305	-31351	11.721	2025	9122

Generally the molecules which have a large dipole moment have a strong asymmetry in the distribution of electronic charge, therefore can be more reactive and be sensitive to change of her electronic structure and electronic properties under an external electric field. Through the table 2, we can observe that the dipole moment (μ) of compounds P2 and P4 are greater than other studied compound, therefore we can say that these compound are more reactive that other compound. In the other side the HOMO and the LUMO energy levels of the donor and acceptor compounds are very important factors to determine whether effective charge transfer will happen between donor and acceptor. The electron-donating ability of the electron-donor in D-π-A dyes has the tendency to influence the electrochemical properties. A D-π-A dye with a stronger electron-donating group should give a high HOMO as compared to that with a weaker electron-donor. We have investigated the electron-donor effect on the electronic properties by using different donor groups. According to the analysis of HOMO, the results of these dyes are in order: P2>P4>P3>P1. The P2 and P4 contains Cl and NO_2 have the highest HOMO (-5.231 and -5.285 eV). Dyes P1 and P3 with calculated HOMO energy levels -5.340, -5.313 eV, respectively, have a weak contribution in electron-donor ability. The calculated LUMO level for all sensitizers are relatively unaffected by the changes in molecular structure, due to the inclusion of same electron acceptor group in these sensitizers, which is less influenced by the change of the donor group. According to the analysis of LUMO, the results of these dyes are in order: P1>P3>P4>P2.

Among parameter influenced on the efficient of solar cells is the V_{oc}, for this in this work we will evaluate the value of V_{oc} of all compounds. The power conversion efficiency (η) was calculated according to the following equation:

$$\eta = FF \frac{V_{oc} J_{sc}}{P_{inc}}$$

Where P_{inc} is the incident power density, J_{sc} is the short-circuit current, V_{oc} is the open-circuit voltage, and *FF* denotes the fill factor.

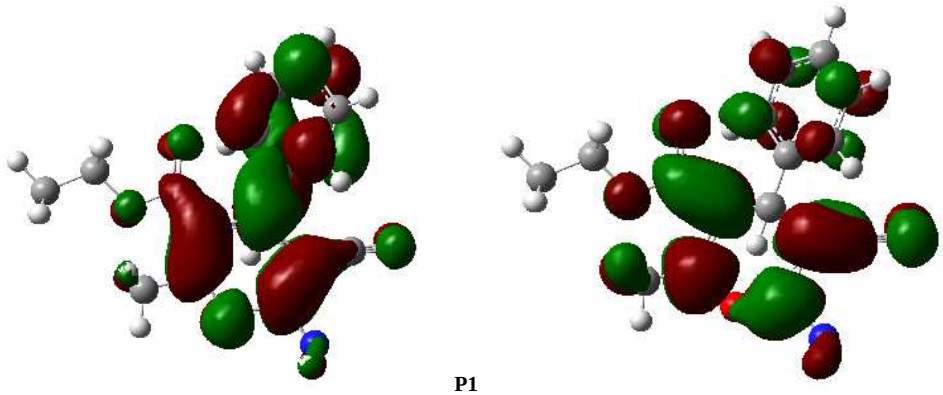

P1

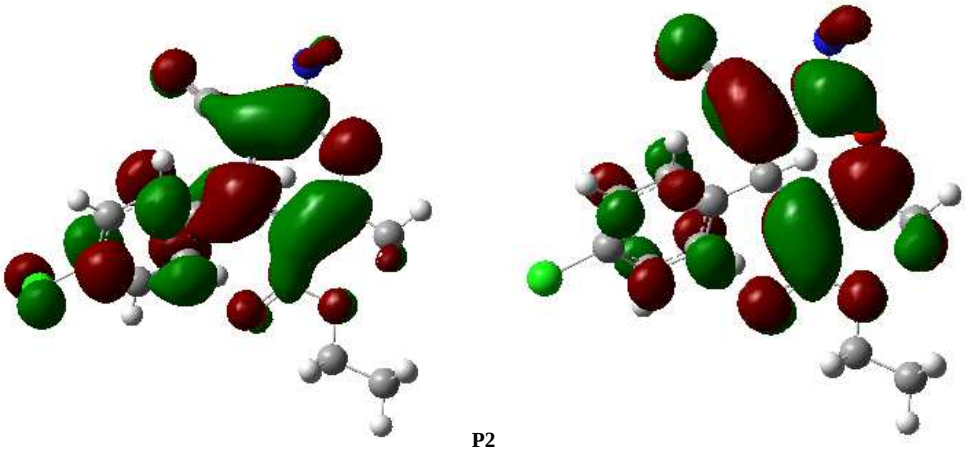

P2

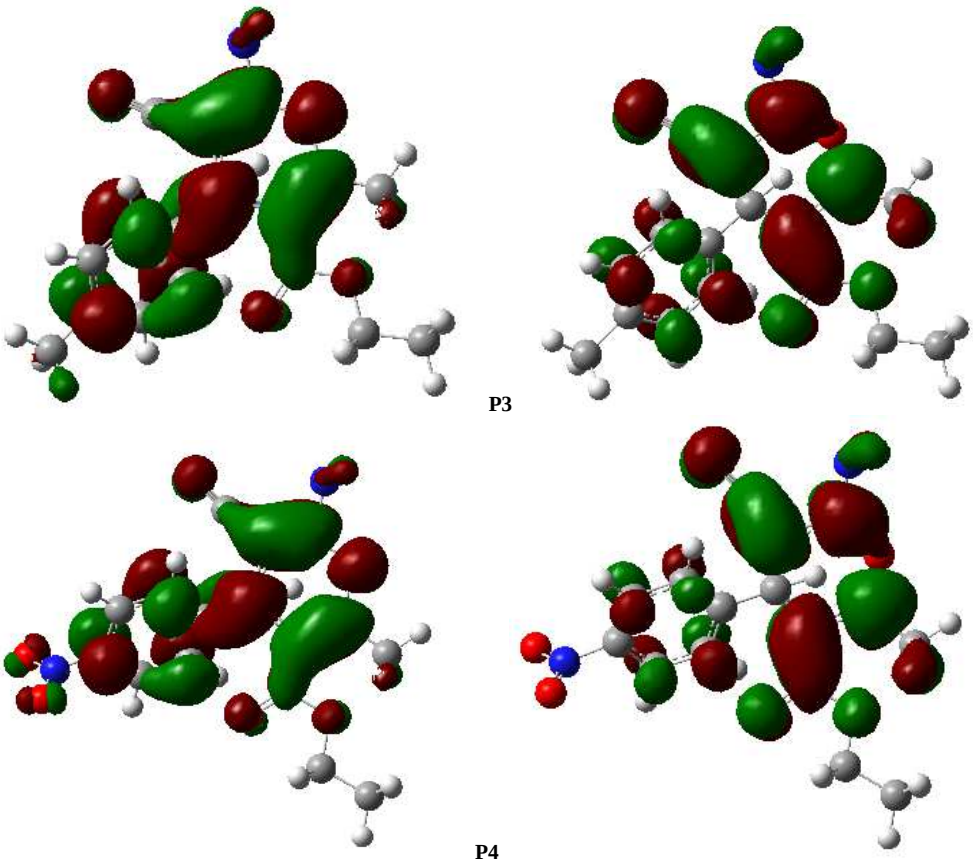

Figure 4: The contour plots of HOMO and LUMO orbital's of the studied compounds Pi

The maximum open circuit voltage (V_{oc}) of the bulk hetero junction (BHJ) solar cell is related to the energy difference between the highest occupied molecular orbital (E_{HOMO}) of the electron donor and the lower unoccupied molecular orbital (E_{LUMO}) of the electron acceptor, taking into account the energy lost during the photo-charge generation [47]. The theoretical values of open-circuit voltage V_{oc} have been calculated from the following expression:

$$V_{oc} = \left|E_{HOMO}^{Donor}\right| - \left|E_{LUMO}^{Acceptor}\right| - 0.3$$

Optical properties

we have calculated the longest wavelength of absorption spectrum (λ_{max}), and corresponding oscillator strength (f) and the vertical excitation energy ΔE (eV) values of four studied compounds Pi (i=1-4). These values are calculated by using TD-DFT/CAM-B3LYP/6-31(d,p) level starting with optimized geometry obtained by DFT/B3LYP/6-31(d,p) level. The obtained results are listed in table 3, which demonstrate that the lowest singlet electronic excitation is characterized as a typical π–π* transition.

Table 3: Absorption spectra data obtained by TD-DFT methods for compounds P1 to P4 at CAM-B3LYP/6-31G (d,p) optimized geometries

Compound	Exited State	Main composition		ΔE (eV)	λ_{max} (nm)	f
P1	S0 → S1	HOMO→LUMO	0.34	2.28	353.64	0.274
P2	S0 → S1	HOMO→LUMO	0.35	2.04	452.56	0.279
P3	S0 → S1	HOMO→LUMO	0.31	2.21	397.82	0.202
P4	S0 → S1	HOMO→LUMO	0.32	2.12	438.14	0.213

The simulated absorption spectra of four compounds are shown in the Fig. 5 and demonstrated that the strongest absorption in UV-visible (λ_{max} > 350nm) correspond to electronic transition HOMO-LUMO of all compounds, but we note that the absorption maxima move by almost 140 nm to the red absorption. The values of λ_{max} of four compounds are in the order of P2>P4>P3>P1, which is in excellent agreement with the corresponding reverse order of E_g values displayed in the precedent section. The increase of a bathochromic shift of four compounds is attributed to increase of the conjugated system of these compounds, especially when going from (P1, P3) to (P4, P2) which

also can be seen respectively in P1 (353.64nm), P3 (397.82nm), P4 (438.14 nm) and P2 (452.56nm), then the effect of the aromaticity and the conjugated system are important to study the electronic and absorption properties of the studied compounds.

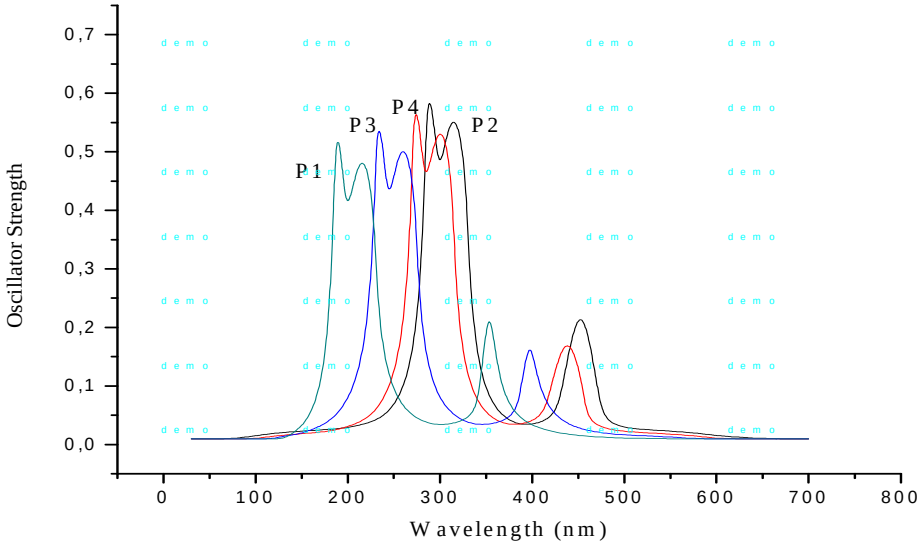

Figure 5: Simulated UV-visible optical absorption spectra of Pi compounds with the calculated data at the TD-DFT/CAM-B3LYP/6-31G (d,p) level

To confirm this result, we determined the dipole moment vectors in a three-dimensional representation of the P1 and its derivatives. Dipole moment μ vectors computed at the RHF/STO-3G level displayed in Fig. 6 lend further support to this image; μ Vectors are referred to the standard orientation of every molecule, i.e. the nuclear charge center for the molecule is at the origin of coordinates.

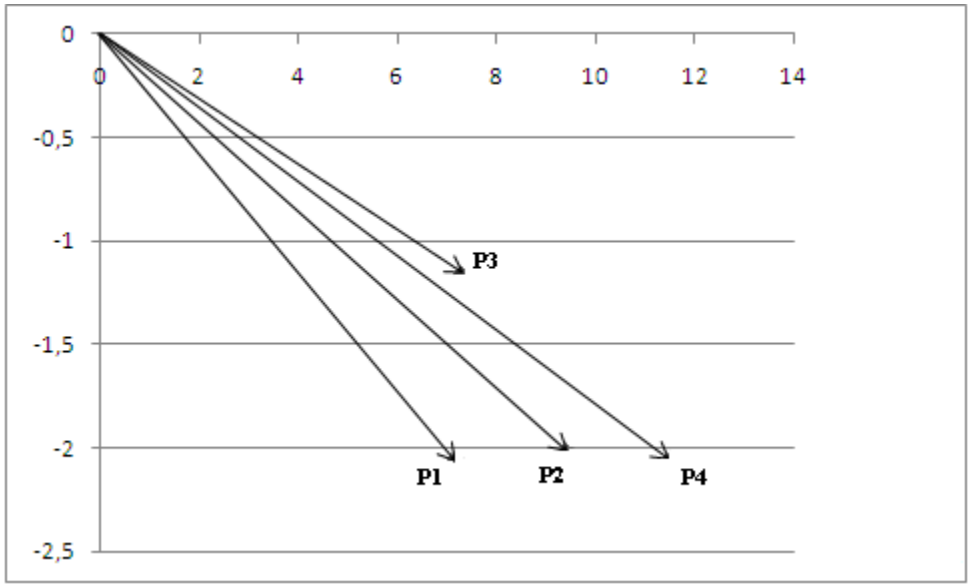

Figure 6: Projection of the dipole moments vector along the z axis, computed at the RHF/STO-3G level of theory for all compounds Pi

We found that the coordinates of the dipole moments of our compounds in 3D are: P1 (7.1518, -2.7567, 0.1862), P2 (9.4276, -2.0134, 0.1941), P3 (7.3102, -1.1591, 0.1580) and P4 (11.5381, -2.0569, 0.1935). The dipole moment for P1 (7.6377 D) is increased when more electronegative substituent Cl and NO_2 are added away from even position in P2 **(**9.6421 D) and P4 (11.7216 D) with an orientation (+8.5° and +13.5°), and decreased when they are replaced in P3 (7.4032 D) by CH_3 substituent in even position and also changes the vector orientation with large angle (+17°). The information provided by NPA charges as well as this change with regard to μ are in agreement with the known weak resonance effect of chlorine, already known [48-51], as compared with its inductive effect.

Photovoltaic properties

The electronic injection free energy ΔG^{inject}, ground E^{dye} and excited E^{dye*} state oxidation potentials computed for our compounds are represented in Table 7. Based on Koopman's theorem, ground state oxidation potential energy is related to ionization potential energy. E^{dye} can be estimated as negative E_{HOMO} [52]. E^{dye*} of all dyes is increasing order: P2<P4<P3<P1. It shows that the most convenient oxidizing species is P2 while P1 is the worst. All ΔG^{inject} estimated is in negative value for all sensitizers, thus the electron injection from the dye to TiO_2 is spontaneous. As seen from Table 4 the calculated ($-\Delta G^{inject}$) are decreased in the order: P2>P4>P3>P1. It shows that P2 has the largest ($-\Delta G^{inject}$) value while P1 has the smallest.

Another factor related to efficiency of DSSC is the performance of the dyes responsible of the incident light. Based on the LHE of the dyes, the value has to be as high as possible to maximize the photocurrent response. The LHE values for all dyes are in narrow range 0.372–0.474 (Table 4), but increase slightly with increasing the conjugation length in the order: P2>P1>P4>P3. This means that all the sensitizers give similar photocurrent.

Table 4: Estimated electrochemical parameters for all compounds

Compound	E_{00} (eV)	E^{dye} (eV)	E^{dye*} (eV)	ΔG^{inject} (eV)	LHE	λ_{total} (eV)	V_{oc} (eV)
P1	2.15	5.34	3.19	-0.81	0.467	0.565	0.022
P2	2.19	5.23	3.04	-0.96	0.474	0.381	0.019
P3	2.13	5.31	3.18	-0.82	0.372	0.501	0.021
P4	2.21	5.28	3.07	-0.93	0.387	0.440	0.020

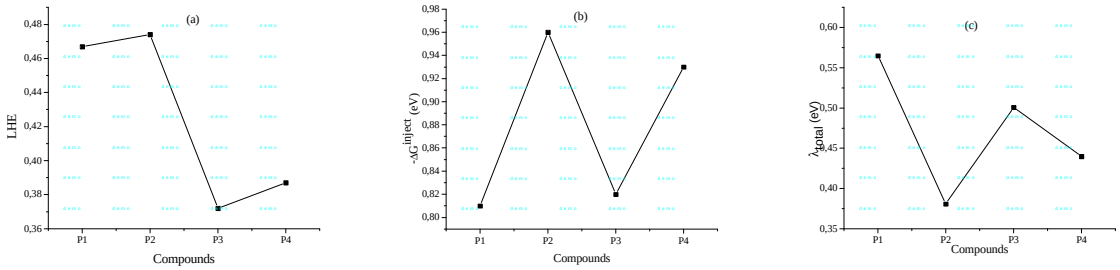

Figure 7: Critical parameters influenced J_{sc} along of investigated sensitizers: (a) the light-harvesting efficiency, (b) the electronic injection free energy, (c) the reorganization energy λ_{total}.

Besides the reaction free energy, the reorganization energy λ_{total} could also affect the kinetics of electron injection. So, the calculated λ_{total} is also important to analyze the relationship between the electronic structure and the J_{sc}. The small λ_{total} which contains the hole and electron reorganization energy could enhance the J_{sc}. As seen from Table 4 and Fig. 7 the calculated λ_{total} of all dyes are increased in the order: P2<P4<P3<P1. It shows that dye P2 possesses the smallest total reorganization energy while dye P1 has the largest. As a result, dye P2 exhibits a favorable J_{sc} due to the relative similar LHE, larger ΔG^{inject} and smaller λ_{total}. At the same time, ΔG^{inject} and λ_{total} are more important to govern the J_{sc} mostly. As discussed in section, we know that besides the short-circuit current density J_{sc} the overall power conversion efficiency η also could be influenced by the open-circuit voltage (V_{oc}). Therefore, between these dyes with similar structures, the electron injection would be more efficient for that dye with the higher excited state related to the semi-conductor conduction band edge (i.e. higher V_{oc}). It was found that V_{oc} of all dyes is in the range 0.019-0.022 eV and in decreasing order: P2<P4<P3<P1. It shows that P1 has the largest V_{oc} values, while P2 has the smallest.

As a consequence of the above data, we could draw a conclusion that the large LHE and ΔG^{inject} as well as small λ_{total} and V_{oc} could have a high efficiency. Thus, the performance of DSSC sensitized by dye P2 might be superior to the other dyes, due to its favorable performances of the above factors based on our computed results.

CONCLUSION

In this study, we used the DFT/B3LYP level to analyze the geometries and electronic properties of new molecules based on pyran with several structures. The modification of chemical structures can greatly modulate and improve the electronic and optical properties of pristine studied materials. The optoelectronic properties of these new conjugated materials have been computed using 6-31G (d, p) basis set at B3LYP level. The concluding remarks are:

• The appropriate functional to predict the electronics properties is B3LYP;
• The appropriate functional to predict the optical properties is CAM-B3LYP;
• The absorption properties have been obtained by using TD-DFT method. The obtained absorption maximums are in the range 353 to 452 nm;

• The calculated band gap (E_g) of the studied molecules was in the range 1.250 to 1.362 eV;
• The calculated values of V_{oc} of the studied molecules range from 0.019 to 0.022 eV.
• The Ethyl 6-amino-4-(4-chlorophenyl)-5-cyano-2-methyl-4H-pyran-3-carboxylate (P2) dye was found to be the best photosensitizer for use in DSSC,

These values are sufficient for an efficient electron injection. Therefore, all the studied molecules can be used as organic solar cells;

Finally, the procedures of theoretical calculations can be employed to predict the optoelectronic properties on the other compounds, and further to design novel materials for organic solar cells.

REFERENCES

[1] V. C. Nguyen, K. Potje-Kamloth, *Thin Solid Films*, **1999**, 338, 142.
[2] R.E. Gill, G.G. Malliaras, J. Wildeman, G. Hadziioannou, *Adv. Mater*., **1994**, 6, 132.
[3] F. Garnier, G. Horowitz, X. Peng, D. Fichou, *Adv. Mater*, **1990**, 2, 562.
[4] G. Wang, S. Qian, J. Xu, W. Wang, X. Liu, X. Lu, F. Li, *Physica*, *Part B*, **2000**, 279, 116.
[5] A. El Assyry, A. Hallaoui, F. Abrighach, R. Touzani, A. Zarrouk, A. Lamhamdi, *Der Pharm. Lett.*, **2015**, 7, 151.
[6] W. Ma, C. Yang, X. Gong, K. Lee, A. Heeger, *J. Adv. Funct. Mater*., **2005**, 15, 1617.
[7] G. Li, V. Shrotriya, J. Huang, Y. Yao, T. Moriarty, K. Emery, Y. Yang, *Nat. Mater*, **2005**, 4, 864.
[8] S. Gunes, H. Neugebauer, N. S. Sariciftci, *Chem. Rev*, **2007**, 107, 1324.
[9] B. C. Thompson, J. M. Frechet, *J. Angew. Chem. Int. Ed*., **2008**, 47, 58.
[10] A. El Assyry, A. Hallaoui, R. Saddik, N. Benchat, B. Benali, A. Zarrouk, *Der Pharm. Lett.*, **2015**, 7, 295.
[11] G. Dennler, M. C. Scharber, C. Brabec, *J. Adv. Mater*., **2009**, 21, 1323.
[12] Zheng Ningjuan, Li Bao, Ma Changwei, Chen Tie, Kan Yuhe, Yin Bingzhu, *Tetrahedron*, **2012**, 68, 1782.
[13] K. R. J. Thomas, J. T. Lin, Y. T. Tao, and C. H. Chuen, *Adv. Mater*., **2002**, 14, 822.
[14] G. Sonmez, C. K. F. Shen, Y. Rubin, and F. Wudl, *Angew. Chem., Int. Ed.*, **2004**, 43, 1498.
[15] M. L. Chabinyc, R. A. Street, J. E. Northrup, *Appl. Phys. Lett*, **2007**, 90, 123508.
[16] E. Bundgaard, F. C. Krebs, *Sol. Energy Mater*., **2007**, 91, 1019.
[17] A. Fitri, A. Touimi Benjelloun, M. Benzakour, M. Mcharfi, M. Hamidi, M. Bouachrine, *J. Spectrochimica Acta Part A*, **2014**, 124, 646.
[18] M. H. Petersen, O. Hagemann, K. T. Nielsen, M. Jorgensen, F. C. Krebs, *Sol. Energy Mater*, **2007**, 91, 996.
[19] A. El Assyry, R. Jdaa, B. Benali, M. Addou, A. Zarrouk, *J. Mater. Environ. Sci*., **2015**, 6, 2612.
[20] Y. A. Sadiki, M. Bouachrine, L. Bejjit, M. Hamidi, S.M. Bouzzine, M. Haddad, F. Serein-Spirau, J. P. Lère-Porte, J. Marc Sotiropoulos, *J . Prog. in Chem. Engin*. **2014**, 1, 1.
[21] A. Zahlou, Y. A. Sadiki, L. Bejjit , M. Haddad, M. Hamidi, M. Bouachrine, *J. Mater. Environ. Sci*., **2014**, 5, 532.
[22] N. Belghiti, M. Bennani, M. Hamidi, S. M. Bouzzine, M. Bouachrine, *J. Mater. Environ. Sci.*, **2014**, 5, 2191.
[23] B. C. Thompson, Y. G. Kim, J.R. Reynolds, *Macromolecules*, **2005**, 38, 5359.
[24] B. C. Thompson, Y. G. Kim, T. D. McCarley, J. R. Reynolds, *J. Am. Chem. Soc*., **2006**, 128, 12714.
[25] E. Bundgaard, C. Frederik Krebs, *Macromolecules*, **2006**, 39, 2823.
[26] Z.L. Zhang, L.Y. Zou, A.M. Ren, Y.F. Liu, J.K. Feng, C.C. Sun, *Dyes Pigm*. **2013**, 96, 349.
[27] J.B. Asbury, Y.Q. Wang, E. Hao, H. Ghosh, T. Lian, *Res. Chem. Intermed*. **2001**, 27, 393.
[28] J. Zhang, H.B. Li, S.L. Sun, Y. Geng, Y. Wu, Z.M. Su, *J. Mater. Chem*. **2012**, 22, 568.
[29] J. Zhang, Y.H. Kan, H.B. Li, Y. Geng, Y. Wu, Z.M. Su, *Dyes Pigm*. **2012**, 95, 313.
[30] W.L. Ding, D.M. Wang, Z.Y. Geng, X.L. Zhao, W.B. Xu, *Dyes Pigm.* **2013**, 98, 125.
[31] W. Sang-aroon, S. Saekow, V. Amornkitbamrung, *J. Photochem. Photobiol. A.* **2012**, 236, 35.
[32] M.P. Balanay, D.H. Kim, *J. Mol. Struct. Thermochem*. **2009**, 910, 20.
[33] S.M. Sze, Physics of Semiconductor Devices, Wiley, **1981**.
[34] A. Ricaud, Photopiles solaires, Presses polytechniques et universitaires romandes, **1997**.
[35] A.D. Becke, *J. Chem. Phys.*, **1993**, 98, 5648.
[36] A. El Assyry, B. Benali, A. Boucetta, B. Lakhrissi, *J. Mater. Environ. Sci.*, **2014**, 5, 1860.
[37] C. Lee, W. Yang, R.G. Parr, *Reviews B*, **1988**, 37, 785.
[38] M.S. Gordon, *Chem. Phys. Lett.*, **1980**, 76, 33.
[39] M.J. Frisch, et al, **2009**, GAUSSIAN 09, Revision B.04. Gaussian, Inc., Pittsburgh PA
[40] X.H. Zhang, L.Y. Wang, G.H. Zhai, Z.Y. Wen, Z.X. Zhang, *J. Mol. Struct.*, **2008**, 881, 117.
[41] D. Mondieig, Ph. Negrier, J.M. Leger, L. Lakhrissi, A. El Assyry, B. Lakhrissi, E.M. Essassi, B. Benali, A. Boucetta, *Russ. J. Phys. Chem. A*, **2015**, 89, 807.
[42] Ph. Négrier, D. Mondieig, J. M. Léger, B. Benali, Z. Lazar, A. Boucetta, A. Elassyry, B. Lakhrissi, C. Jermoumi, M. Massoui, *Anal. Sci.*, **2006**, 22, 175.

[43] B. Benali, Z. Lazar, K. Elblidi, B. Lakhrissi, M. Massoui, A. Elassyry, C. Cazeau-Dubroca, *J. Mol. Liq.*, **2006**, 128, 42.
[44] A. El assyry, B. Benali, A. Boucetta, Z. Lazar, B. Lakhrissi, M. Massoui, D. Mondieig, *Spectrosc. Lett.*, **2009**, 42, 203.
[45] B. Benali, A. El Assyry, A. Boucetta, Z. Lazar, B. Lakhrissi, M. Massoui, D. Mondieig, *Spectrosc. Lett.*, **2007**, 40, 893.
[46] A. Elassyry, B. Benali, Z. Lazar, K. Elblidi, B. Lakhrissi, M. Massoui, D. Mondieig, *J. Mol. Liq.*, **2006**, 128, 46.
[47] A. Gadisa, M. Svensson, M.R. Andersson, O. Inganas, *Appl. Phys. Lett*., **2004**, 84, 1609.
[48] A. El Assyry, B. Benali, A. Boucetta, D. Mondieig, *Res. Chem. Intermed.*, **2014**, 40, 1043.
[49] A. El Assyry, B. Benali, *Res. Chem. Intermed.*, **2014**, 40, 627.
[50] Z. Lazar, B. Benali, K. Elblidi, M. Zenkouar, B. Lakhrissi, M. Massoui, B. Kabouchi, C. Cazeau-Dubroca, *J. Mol. Liq.*, **2003**, 106, 89.
[51] A. El Assyry, B. Benali, A. Boucetta, B. Lakhrissi, *J. Struct. Chem.*, **2014**, 55, 38.
[52] R.G. Pearson, *Inorg. Chem.*, **1988**, 27, 734.